Title:

The influence of graphene oxide filler on the electrical and thermal properties of unidirectional carbon fibre/epoxy laminates: effect of out-of-plane alignment of the graphene oxide nanoparticles

Authors List:

Evangelos C. Senis[1], Igor O. Golosnoy[1], Thomas Andritsch[1], Janice M. Dulieu-Barton[2] and Ole T. Thomsen[2]

[1]Faculty of Engineering and Physical Sciences, University of Southampton, Southampton, United Kingdom

[2]Bristol |Composites Institute, University of Bristol, United Kingdom

Corresponding author: Evangelos C. Senis, e-mail: e.senis@soton.ac.uk

Abstract

The influence of out-of-plane alignment of Graphene Oxide (GO) platelets used as matrix filler on the through-thickness electrical and thermal conductivity of unidirectional (UD) carbon fibre reinforced polymers (CFRP) composites has been investigated. By utilising an external AC field, the orientation of GO flakes was altered to take advantage of the higher electrical and thermal conductivity along the graphene basal planes. Commercially available GO was dispersed in quantities up to 5 wt% into the epoxy matrix prior to vacuum infusion into dry carbon fabric to form CFRP laminates. Both GO modified CFRP laminates containing randomly oriented GO and aligned GO modified CFRP (A-GO/CFRP) laminates were manufactured to assess the influence of the application of the electric field. Measurements of the electrical conductivity revealed markedly increased values for the A-GO/CFRP even with low filler contents. The thermal conductivity, albeit increased in A-GO/CFRP, only resulted in modest improvements. Mechanical tests of the interlaminar shear strength (ILSS) showed that the A-GO/CFRP laminates exhibited significantly improved behaviour and retained higher ILSS values (than the randomly aligned GO CFRP laminates) even at high filler contents.

1 Introduction

The addition of nanofillers to fibre reinforced polymers (FRPs) as a means to improve their mechanical response, and lately to introduce functionality, mainly enhancing their electrical and thermal properties, has been a major research focus point over the last decade [1,2]. By incorporating a secondary reinforcing phase, a multi-scale composite with improved properties can be realised. It is known that the type of filler, content, shape and size have a strong influence on the properties of nanocomposites. Fillers with high aspect ratios, e.g. platelets and rods/tubes, are known to be more efficient than traditional particle shaped filler systems [3,4]. For the particular case of the through-thickness conduction in FRP composites, improving the electrical and thermal properties relies on facilitating the conduction through the polymer rich interlaminar regions [5–8].

To do so, fillers are usually incorporated/dispersed into the polymer matrix aiming to assist the conduction process either by being dispersed in the bulk of the laminate [6,9–11] or by nanostructuring the interlaminar regions [5,12]. The objective of all of these approaches is to interconnect the adjacent laminae through a percolating network of conducting fillers. However, parameters such as the state of agglomeration, the geometry and aspect ratio of the filler as well as the viscosity of the matrix, to name some, influence the particle network structure. High electrical and thermal conductivity can only be realized by reaching percolation, i.e. by forming a continuous network through the bulk of the system [13–15]. However, high filler contents are required, leading to poor material processability and mechanical properties, higher cost and added complexity. Thus, new methods of controlling the spatial arrangement of filler needs to be employed to successfully incorporate and promote the use of nanofillers in advanced composite structures. The use of electric and magnetic fields to align or orient carbon nanotubes (CNTs) has shown great potential in enhancing the electrical and thermal conductivity in recent research [16,17]. Due to the lower amount of filler

required to create a conducting network within a polymer these methods have shown great potential for commercial applications. However, magnetic fields are impractical in view of industrial exploitation because of the increased complexity and high fields needed, ≥5T [16,18,19]. On the other hand, electric fields require simpler setups, both AC and DC fields have been used in literature and for different material systems to create a nanostructured network by either controlling the filler orientation [17,20–24] or to deposit the filler in specific locations [25,26]. In addition, electric field alignment is scalable and has shown its potential for several applications such as electrostatic charge dissipation [27,28].

Although the concept of aligning some types of nanofiller systems into composite laminates, as a means to improve the interlaminar fracture toughness, has been investigated in the past [21], new requirements for CFRP laminates in areas where high thermal loads and electrical current are part of the operational environment are becoming increasingly important.. It is known that CFRP laminates exhibit poor through-thickness properties (mechanical, electrical and thermal) limiting or even hindering their incorporation into structures for some applications. To address this weakness several methods have been introduced over recent years; from Z-pinning [29,30] and through-thickness stitching in woven fabrics [31], to the addition of nano sized inclusions into the polymer matrix [10,32], or by modifying the fibre surface [33,34]. Applications such as lightning strike protection, heat exchangers and anti/de-icing, to name a few, require increased through-thickness electrical and thermal conductivity to mitigate potential damage to the composite structure [8,35]. The key difference related to nanomodified CFRP with continuous carbon fibre reinforcement as opposed to polymer nanocomposites, is that for the former the polymer matrix needs to have a very low viscosity, thus not in percolating state, to allow the nano particle filled matrix to infiltrate the continuous fibre fabric to enable successful consolidation of the laminate.

This study investigates the use of an applied AC electric field during the curing of UD CFRP laminates containing GO dispersed within the epoxy matrix. This strategy was chosen as a means of orienting the GO flakes perpendicular to the fibre direction aiming to form a conducting network interconnecting the carbon fibres in the laminae. Of particular interest is to correlate the influence of the GO alignment to the required amount of GO needed to improve the electrical and thermal properties, as is critical for commercial/industrial applications. Furthermore, the interlaminar shear strength (ILSS) will be measured to assess the influence of GO nanofiller content on the mechanical properties of the laminate. Specifically, the objectives of this work are to:

- Develop a manufacturing method for GO-modified CFRP laminates that is scalable and thus applicable to the composites industry, and which aligns the GO filler perpendicular to the carbon fibres.
- Determine the influence of the GO alignment process on the electrical, thermal and mechanical properties and compare it with the behaviour of laminates containing randomly oriented GO.
- Examine the effect of the alignment process on the GO filler content required to achieve improved electrical, thermal and mechanical performance.

2 Experimental

2.1 Materials

A two-component epoxy system kindly supplied by Leuna Harze, Germany, was used as matrix material. The system consisted of EPILOX® ER 5300 epoxy resin and EPILOX® EC 5310 curing agent with a viscosity of 275 mPa.s. The components were mixed by weight at a ratio of 100/20 according to the specifications of the manufacturer. The Graphene Oxide (GO)

(edge-oxidized) was kindly provided by Garmor Inc, USA, consisting of approximately 10 graphene layers and a nominal particle size diameter of 500nm, 90% of the particle sizes below 800 nm, with an Oxygen content in the range of 5-10%, according to the GO supplier. A unidirectional (UD) non-crimp carbon fabric, with Zoltek Panex 35 carbon fibres and an areal mass density of 882 g/m^2, was used as reinforcement. The composition of the fabric consisted of 852 g/m^2 Zoltek Panex 35 carbon fibres, 24 g/m^2 of E-glass and 6 g/m^2 of PES, and E-glass and PES (Polyester) were used for stitching purposes.

2.2 Manufacturing of aligned GO modified CFRP laminates

The manufacturing procedure of the aligned GO modified CFRP and randomly oriented GO modified CFRP laminates is presented in Fig.1. Unidirectional laminates were manufactured based on a previously developed method [6]. The dispersion of GO into the epoxy was realised by means of high speed planetary mixing, Flacktek Speedmixer™ DAC 150.1 FV, for 5 min at 3000 rpm at ambient temperature. This method has been proven to provide good dispersion of carbonaceous nanoinclusions in epoxy and has been used in previous work [6,36]. After the mixing, the curing agent was added and the mixture was hand stirred for 5 min followed by degassing at ambient temperature. Due to the high areal weight of the reinforcement, and to resemble conditions similar to industrial applications like e.g. wind turbine blade laminates, the Vacuum Assisted Resin Infusion Method (VARIM) process was used. The resin inlet channel was positioned along the fibre direction. The composition of the manufactured laminates is listed in Table 1. To assess the influence of the applied electric field on the orientation of GO flakes, and consequently the through-thickness electrical and thermal conductivities, two series of specimens were manufactured, series one consisted of laminates containing randomly oriented GO (GO/CFRP) and series two AC field oriented GO (A-GO/CFRP), respectively. The carbon fibre volume fraction was the same for both laminate types and it was approximately 57 ±2%. After the infusion process, the laminates were cured

for 6 h at 70 ºC following the suggested curing profile from the resin supplier. During the curing an external electric field was applied as described in Section 2.3.

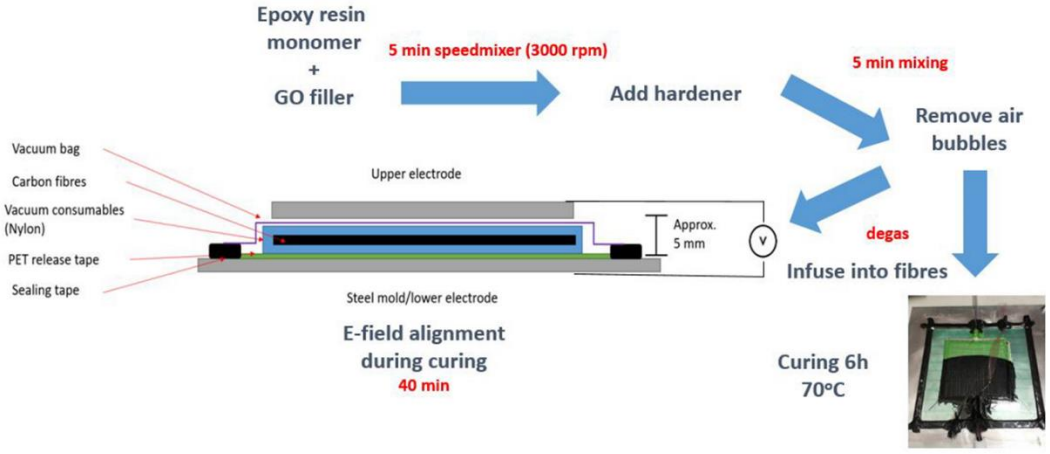

Fig.1: Schematic of the manufacturing route for the GO/CFRP and A-GO/CFRP laminates.

Table 1: Composition of manufactured laminates

Sample/ wt% of GO in the matrix	$V_{GO(matrix)}$%	$V_{GO(laminate)}$%	V_f%
Unfilled	0	0	57
0.5	0.32	0.14	57
1	0.63	0.27	57
2	1.26	0.54	57
3	1.89	0.81	57
4	2.52	1.08	57
5	3.15	1.35	57

2.3 Aligning GO in CFRP laminates

The theory describing the mechanism of the electric-field-induced alignment of nano-sized filler material in a polymer medium is well documented for a wide variety of fillers [17,20,21,37–41]. Briefly, when a sinusoidal alternating field is applied to a conductive rod or platelet-like inclusion located in a dielectric liquid, a dipole moment is created due to charge accumulation around its edges, Fig.2. This polarization is generated due to the difference in

electric conductivity between the dielectric liquid and the inclusion. Due to their shape, platelet inclusions exhibit higher polarization parallel to the platelet surface than the direction normal to their plane. This allows platelets to be oriented with the lateral dimension parallel to the applied field. For the case of Graphene-based inclusions, this direction aligns with the axis of higher conductivity, as it is parallel to the graphene basal planes. In conjunction, the accumulation of opposing charges on the edges of the platelet favours the formation of chains-like networks, as attractive forces between opposing charges interconnect adjacent platelets. The advantage of this mechanism/method is the formation of a percolating network without the necessity for the composite system to be already in the percolating phase. This can be beneficial for the processability of nano-particle filled polymer matrixes since percolating systems exhibit higher viscosity, thus hindering their use in infusion/moulding processes.

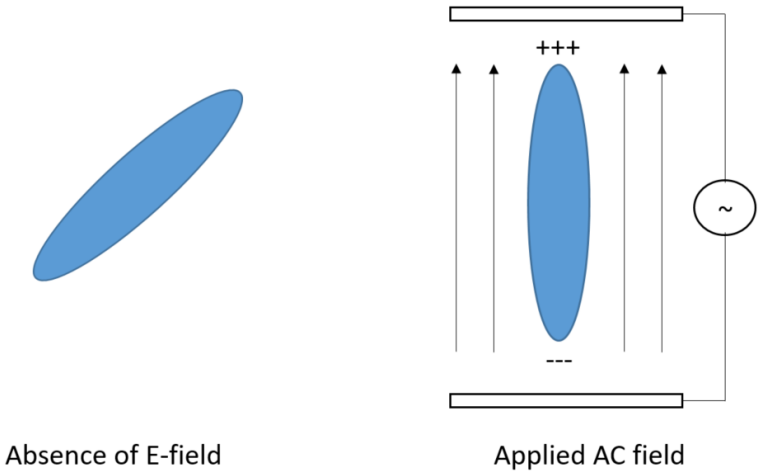

Fig.2: Alignment process of a platelet type filler by the induced AC field

To align the GO flakes into the bulk of a composite laminate a capacitor-like configuration was created based on the mould used for the infusion of each laminate. One major concern when applying an electric field to an epoxy resin in liquid state is the higher conductivity that epoxies exhibit compared to when is in its solid state [42,43]. Hence, current flow needs to be eliminated to avoid resistive heating phenomena. Thus, a PET tape was

applied to the mould surface to electrically separate/insulate the laminate from the mould. A second electrode was placed outside of the vacuum bag to avoid direct contact with the liquid matrix. A sinusoidal wave voltage signal was applied to the electrodes through a TTi TG1010A function generator connected to a TREK PZD 700A high voltage amplifier. The field parameters, 30 V/mm at 10 kHz, were chosen based on previous studies conducted for epoxy systems containing graphene nanoplatelets (GNPs) with similar Oxygen content [17], as well as other carbonaceous inclusions dispersed in polymer matrixes [21,44]. The application time, 40 min, was determined based on the epoxy viscosity development with temperature during the curing process (information provided by the resin supplier).

2.4 Experimental methods

To estimate the through-thickness electrical conductivity of the GO/CFRP and A-GO/CFRP, DC resistance measurements were realised with a two-probe setup using a TTi BS-407 precision milli/micro-ohmmeter. During the measurements the applied electrical current was 5 mA. Circular disk shaped samples with a diameter of 50 mm and a thickness of approximately 4 mm were cut from the manufactured CFRP plates. Prior to being measured the sample surfaces were sanded to remove excess epoxy and expose the carbon fibres. Finally, a silver paste with a bulk conductivity of 10^3 S/cm, supplied by RS Components, UK was applied to mitigate surface roughness and assure ohmic contact between the sample and the electrodes. To promote reproducibility, 5 MPa of external pressure were applied to the electrical contacts through a hydraulic press. The conductivity of the composites is above 0.01 S/m along all principle directions, and the characteristic time RC is below 1 ns. The power supply was switched on manually and the readings are taken 30 sec afterwards.

The thermal conductivity was measured using a steady-state technique based on the guarded hot plate method. For both electrical and thermal conductivity measurements, at least 2 samples were tested per filler content. A detailed description of the methods and testing

protocols used for the characterization of the electrical and thermal conductivity can be found elsewhere [6].

Short beam shear tests, 3-point bending, were performed in accordance with the ASTM D2344 test standard to evaluate the interlaminar shear strength (ILSS) and the resistance to crack initiation of the manufactured samples [45,46]. An Instron 5569 universal electro-mechanical testing machine with a load capacity of 50 kN was used for the mechanical tests. The crosshead movement rate of the mechanical testing machine used was 1 mm/min, and the span to width ratio was set to 4:1, according to the ASTM standard. To account for discrepancies from the infusion process of the GO-modified epoxy into the carbon fabric, samples were cut both near the resin inlet and vacuum outlet sides, at least 5 samples per GO content were measured. The obtained results are quoted as the mean of the values obtained for the resin inlet and vacuum sides, all samples were cut from the same plate. Finally, the microstructure and morphology was examined by means of optical microscopy; an Olympus BX-51 optical microscope, and a scanning electron microscopy (SEM), Carl Zeiss EVO 50, were used. To assist the identification of the observed features during the optical microscopy, Raman spectra were obtained using a Renishaw RM100 confocal microprobe system operating at 6.25 mW power with 780 nm laser excitation. The magnification of the objective lens was x50, giving a beam spot diameter of approx. 5 μm.

3 Results

3.1 Morphology

3.1.1 Optical microscopy

In Fig.3 an optical micrograph of the interlaminar region of the sample containing 4 wt% A-GO/CFRP is presented. In addition to the carbon fibres, in the upper and bottom parts of the micrograph, smaller objects are observed dispersed within the interlaminar region. To verify

their identity Raman spectroscopy was utilised. By initially obtaining a spectrum from pure GO nanopowder a baseline was established. Considering that the spot size of the laser was 5 μm, mapping of the area depicted in Fig.3 was realised. By focusing the laser beam to the spot (a), an area with 4 visible features, a spectrum was obtained. Two characteristic bands are observed at 1307 and 1578 cm^{-1}, namely D and G, where D represents the extent of disorder, while G represents the in-phase vibrations of the sp^2 carbon lattice and is associated with the first-order scattering of E_{2g} phonons [47–49]. By obtaining a spectrum from spot (b), which corresponds to an area with no visible features, a near amorphous behaviour was observed, with some indications of a crystalline structure to be present, possibly originating from GO flakes located deeper than the top surface.

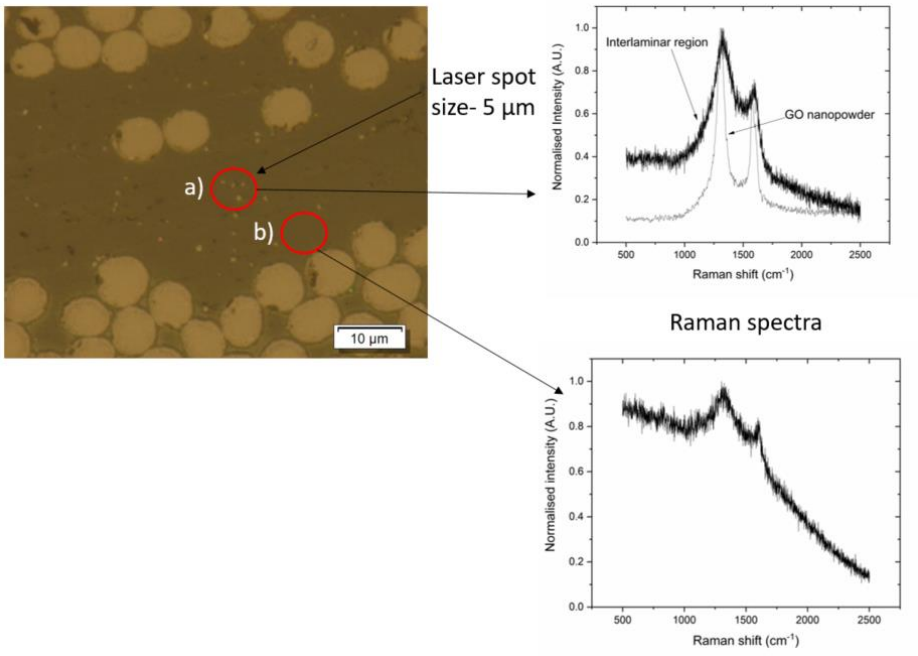

Fig. 3: Optical micrograph from the sample 4 wt% A-GO/CFRP and respective Raman spectra. Red circles denote the areas the spectra where obtained from.

3.1.2 SEM

The morphology, as examined by means of electron microscopy, is presented in Fig. 4. On the left hand side, SEM images corresponding to A-GO/CFRP are depicted, while on the right hand side GO/CFRP are presented. For the samples that were exposed to the applied field (A-GO/CFRP) the GO flakes appear to be arranged in a chain-like configuration, unlike the GO/CFRP samples were the GO flakes are randomly dispersed/oriented. The observed alignment with the applied AC field has caused the formation of physical contacts/paths between adjacent GO flakes and appear to interconnect fibres as seen in Fig.4 a and Fig.4 c. In the two bottom images (Fig.4 e and Fig.4 f) fractured areas from ILSS tests are presented. GO particles are oriented perpendicular to the fibre direction, Fig 4 e, unlike in the random GO/CFRP, Fig. 4 f, where the GO platelets appears to be mainly oriented parallel to the fibre direction.

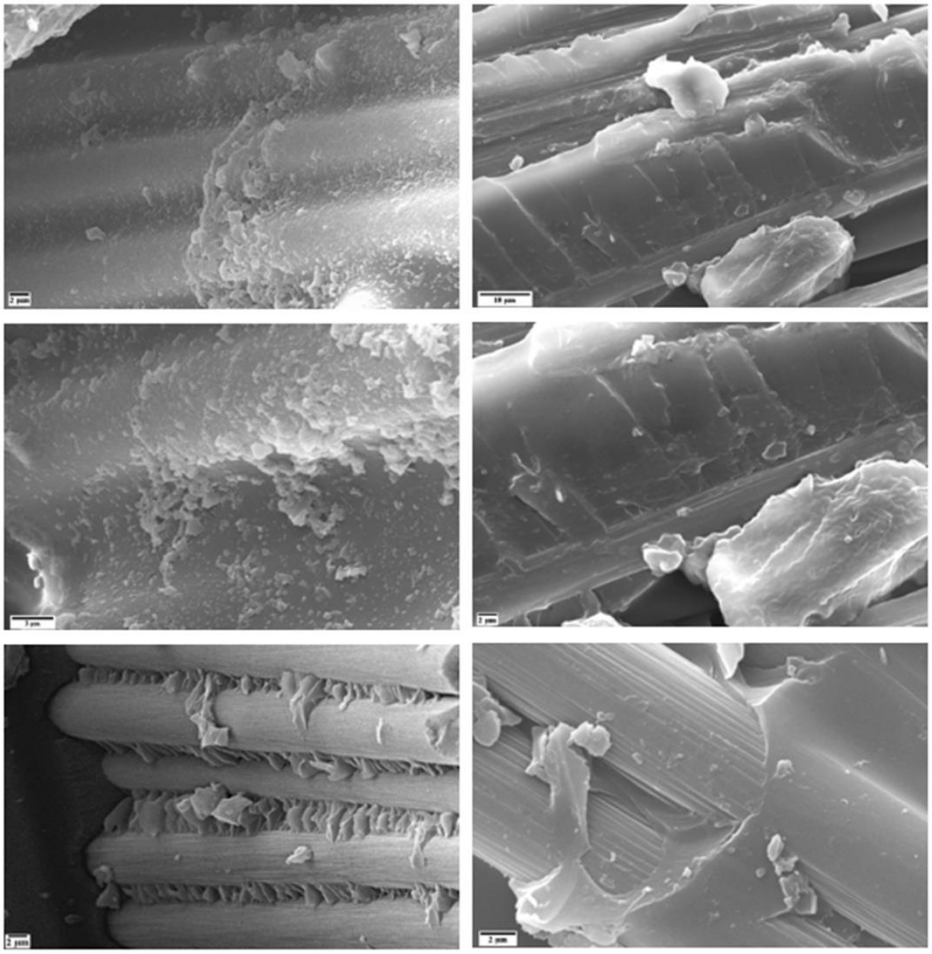

Fig.4: Scanning electron microscopy images for the samples containing 4 wt% GO a), c) and e) (aligned GO) and b), d), f) (randomly oriented GO), bottom images correspond to ILSS fractured topographies.

3.2 Electrical conductivity

Fig. 5 shows the dependency of the through-thickness electrical conductivity on the GO filler content for laminates containing randomly oriented GO and GO aligned perpendicular to the fibre direction. Noticeable improvements are observed for the laminates where the AC field is applied compared to the laminates containing randomly oriented GO. By comparing samples featuring the same GO filler content, the influence of the E-field alignment can be assessed. Although the effects of out-of-plane alignment seem to be pronounced from filler contents above 1 wt%, a 14% increase is observed even for the sample containing 0.5 wt% GO dispersed

into the epoxy. For higher filler contents, the response of the A-GO/CFRP shows improvements ranging from 52% for the 1 wt% sample, 34% for 2 wt%, 68% for 4 wt% and 67% for the 5 wt% sample respectively. As seen the highest observed value, 5 wt% sample, of 0.16 S/cm shows a threefold increase over the neat CFRP laminate.

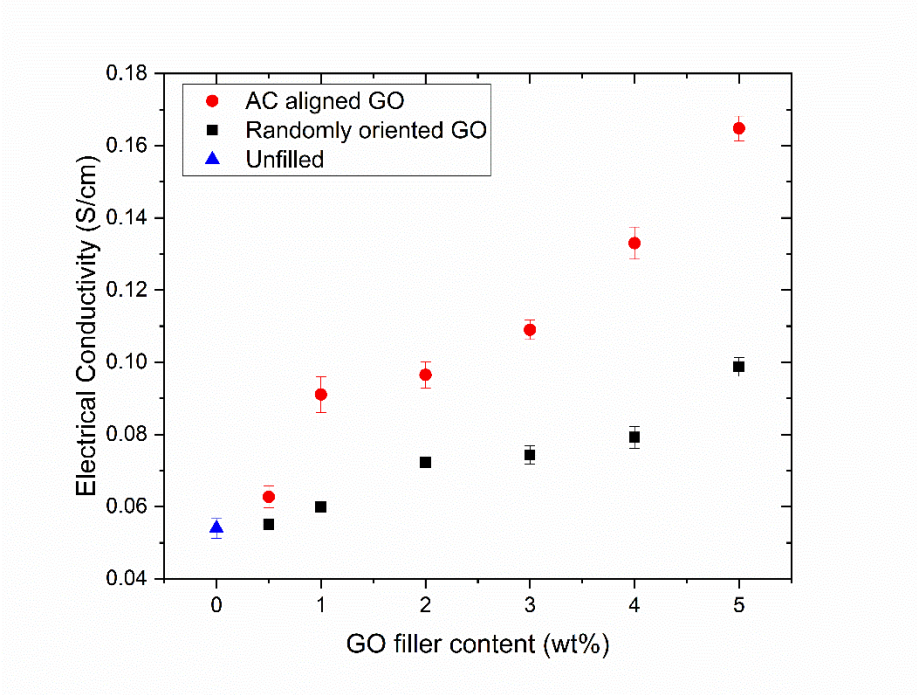

Fig.5: Comparison of the through-thickness electrical conductivity for GO/CFRP and A-GO/CFRP as a function of GO filler content.

3.3 Thermal conductivity

The through-thickness thermal conductivity of both GO/CFRP and A-GO/CFRP is presented as a function of the GO filler content in Fig.6. The addition of GO provides significant improvements in the thermal conductivity for both laminate types. Specifically, continuous increase is observed for low filler contents, 0.5 wt%, 1 wt%, 2 wt% and 3 wt%. Further increase of the filler content provides some marginal improvements with the measured

values appearing to stabilize, reaching a plateau at about 4 wt%, with the exception of the sample containing 5 wt% where a slight decrease is recorded.

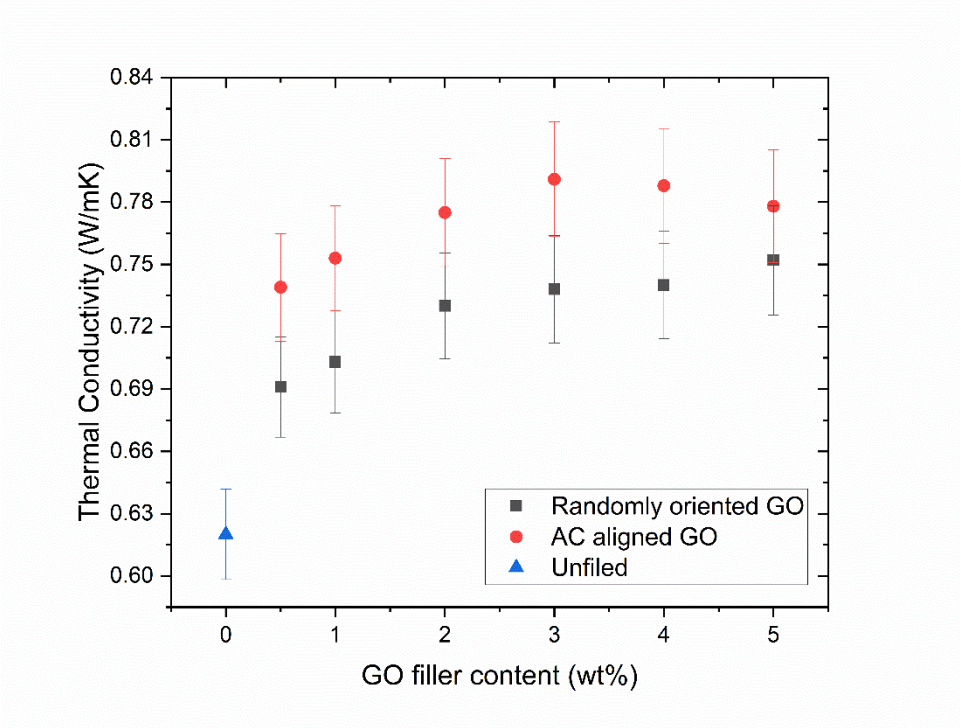

Fig. 6: Through-thickness thermal conductivity for A-GO/CFRP and GO/CFRP as a function of the filler content. The vertical axis is focus on the values between 0.55 and 0.85 W/m/K, giving a magnified view on the region of interest. The experimental errors are within the range of ±5% that is typical for steady state thermal conductivity measurements.

3.4 ILSS

The interlaminar shear strength results measured for the A-GO/CFRP are presented and compared with CFRP laminates containing randomly oriented GO in Fig.7. As suggested by the results, the addition of low filler contents of GO, 0.5 wt% and 1 wt%, leads to a sharp increase in the ILSS for both laminate types. Although the obtained values for the 1 wt% are quite similar, the laminate containing aligned GO shows slightly lower values, but it is within the measurements uncertainty. For the lowest percentage of GO, 0.5wt%, a 20% increase is

observed for the A-GO/CFRP laminate compared to the conventionally GO infused laminate. A similar behaviour is exhibited for filler contents of 2 wt% and 4 wt%, with the laminates containing aligned GO seen to exhibit 56% and 30% improved ILSS, respectively. Further increase of the GO content, 5 wt%, decreases the ILSS of the AC aligned laminates while some minor improvements are seen for the laminates containing randomly oriented GO.

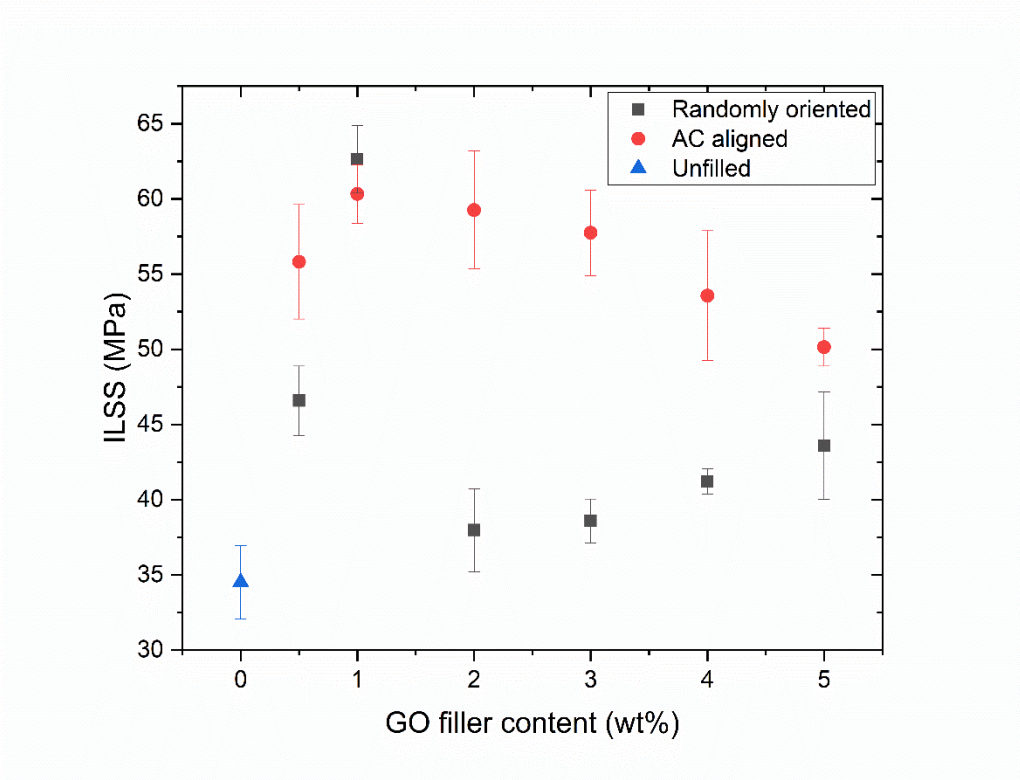

Fig.7: Interlaminar shear strength as a function of GO filler content for the GO/CFRP (randomly oriented) and A-GO/CFRP (AC aligned).

4 Discussion

4.1 Sample Morphology

As seen in the optical micrograph presented in Fig.3, several features are observed within the resin rich interlaminar region of CFRP laminate. Based on their size, i.e. sub-micron diameter, they can be categorised as GO flakes. From the embedded Raman spectra, it can be observed that the features located in the interlaminar region consist of GO. From the spectrum

obtained from the area with no visible features a near amorphous behaviour is observed, as expected for the epoxy matrix. However, an indication of the existence of GO was observed with the formation of weak D and G bands. This can be attributed to the existence of GO located further deeper under the surface that was excited from the laser ray, as the penetration depth of such lasers can be in the range of hundreds of nm [5]. In addition, due to the development of electrostatic attractive forces between the opposing charges of adjacent polarised GO flakes a chain-like network is expected to be formed [17]. Although some indications of this network type can be observed in Fig.3, they are not conclusive, firstly because optical micrographs provide information only about a specific plane and secondly the surface preparation route, surface polishing with abrasive sandpapers, have probably removed some of the GO that was located on that plane. SEM micrographs are presented in Fig.4 (left). There the formation of physical chain-like conducting paths between adjacent fibres is observed. The morphology of the observed features, chain-like network, is similar to previously reported networks consisting of GNPs dispersed in epoxy [17] and clay dispersed in polydimethylsiloxane (PDMS) [20] that were subjected to out-of-plane alignment with an external AC field. In addition, a clear indication of a successful alignment process is evident as the GO flakes appear to be oriented perpendicular to the fibre plane, thus in parallel with the direction of the applied field. This is expected to have a significant influence on both the electrical and thermal conductivity for two distinctive reasons; the formation of such percolating type of network is essential in order to promote the conduction process within the insulating epoxy matrix. Furthermore, since GO flakes are oriented with their basal planes positioned in parallel with the direction of applied electric current and heat flow, both conduction processes will be facilitated by taking advantage of the higher electrical and thermal conductivity of GO in this direction parallel to the basal planes. Samples containing randomly oriented GO, Fig.4 (right), show a different morphology. Albeit the flakes appear to be finely dispersed within the epoxy matrix, no percolating/physical

path can be detected. This also becomes apparent in Fig. 4 were ILSS fractured areas are observed.

4.2 Electrical conductivity

The efficiency of altering the orientation of GO flakes with the external field can be quantified by comparing the through-thickness electrical conductivity values between laminates with the same GO filer content. As depicted in Fig.5 laminates that were subjected to the AC-field alignment process show a sharper increase in conductivity over laminates containing randomly oriented GO. The effects are evident even from low filler contents, 1 wt% and 2 wt%, where an increase of 52% and 34% is seen, respectively, bringing the conductivity values close to 0.1 S/cm. Further increase of the GO filler content leads to an even higher rate of improvement for the A-GO/CFRP. This is directly linked with the ability to form a network among the dispersed GO flakes as the filler content gets higher. Albeit the alignment facilitates the current conduction along the higher conductivity axis of GO, the existence of physical conducting paths observed in higher filler contents, as demonstrated in Fig. 4, dominate the conduction process. At low filler contents, up to 2 wt%, the number of GO flakes/particles in not sufficient to initiate the formation of a network due to long distances between the particles allowing only a small amount of paths/segments to be created. However, as the filler content increases the interparticle distances are being reduced, and thus the assembly of an additional percolating network/path is facilitated. In addition, the formation of large aggregates is impeded due to repulsive forces between the GO flakes. It has to be pointed out that in previously reported results with identical constituent materials [6], to achieve through-thickness electrical conductivity values in the range of 0.18 S/cm, double the amount of GO had to be dispersed into the epoxy, around 10 wt%, showing the efficiency of the AC field alignment method over randomly distributed conducting particles.

It is worth to note that the percolation exists even in the neat composite. In CFRP laminates the percolation threshold can be found around 45% fibre volume fraction. The laminates manufactured in this study had a fibre volume content of approximately 57% thus well above the threshold. Even epoxy reach inter-laminar regions contain several irregular fibre contacts points, although at significantly lower extend in comparison to those inside the laminates. Electric conductivity of the inter-laminar region has been estimated on the sample containing of 5 layers of carbon fabric and 4 inter-laminar regions. We assume that the majority of the GO particles stay within the inter-laminar regions and do not penetrate within the laminae. In this case the conductivity of a single lamina is approximately equal to the conductivity of the composite in the transverse direction, in our case σ_t=0.56 S/cm [6]. Consider an ideal case where no fibre waviness takes place and clearly defined inter-laminar regions are formed with the thickness of approximately 40 microns. The inter-laminar resistance can be calculated assuming the resistors in series with results summarised in Table 2. The epoxy rich layer in the neat CFRP has a conductivity of around 0.002 S/cm, well above the epoxy resin conductivity. So there is a percolation between the laminae, but it can be enhanced further by the addition of GO flakes. As seen from the values listed in the table, the samples exposed to AC alignment exhibit double the inter-laminar conductivity compared to CFRP containing randomly oriented GO, for the same filler content.

Table 2: Effects of GO flake and their alignment on the electric conductivity of epoxy-rich inter-laminar regions, R_t is the total resistance of the sample, R_{int} is the resistance of a single interlaminar region and σ_{int} the corresponding conductivity.

Sample	$R_t(\Omega)$	$R_{int}(\Omega)$	σ_{int}(S/cm)
Neat	0.51	0.118	0.00173
4wt%	0.370	0.0828	0.00246
4wt%_AC	0.202	0.0408	0.00499

4.3 Thermal conductivity

The through-thickness conductivity was measured using a steady-state technique based on the guarded hot plate method [6]. The obtained results are reliable with the uncertainty to be found to be approx. 5%. This level of uncertainty is common for steady-state measurements in polymer and fibre reinforced polymer composites[50], with lower uncertainties exhibited only by transient plane source methods[51]. Commonly used laser flash method often provide higher degree of uncertainty[10]. As seen in Fig. 6 the out-of-plane alignment of the GO provides noticeable improvements in the through-thickness conduction. The effects are visible even from low filler contents, 0.5 wt% and 1 wt%, while reaching the maximum value at 3 wt% GO filler content. A similar trend is also observed for the laminates containing randomly oriented GO. The main mechanism describing the enhancement in the through-thickness direction is the faster heat diffusion through the polymer dominated interlaminar regions due to the higher thermal conductivity of GO [6]. Albeit the addition of a thermally conductive filler will promote higher thermal conductivity values, the platelet-shaped GO fillers exhibit a certain degree of anisotropy, with considerably lower conductivity in the out-of-plane direction [4,52]. In addition, it has been found that the processing/manufacturing procedure have an effect on the filler orientation; platelets have been found to be aligned parallel to the injection direction during the molding process of a polymer composite [52]. Based on previous studies [17,20,52], the thermal behaviour exhibited by randomly oriented platelets dispersed within a polymer matrix, closely resembles the behaviour of platelets aligned in-plane (platelets aligned perpendicular to the heat flow), thus explaining the lower values observed in the absence of the electric field. For the case of A-GO/CFRP further addition of GO contributes to possible irregular chain formation. This has been reported to not efficiently improve the thermal conductivity, as the formation of aggregates reduces the ability to conduct heat effectively through the bulk of the surrounding polymer [53]. Furthermore, one significant aspect affecting the thermal conductivity

of graphene-filled polymer composites is the influence from the interface contact resistance between the filler and the epoxy matrix as well as between the filler particles when in contact [54]. Albeit the alignment facilitate the phonon transport along the GO basal planes the fact that the GO flakes are arranged in a chain-like network increase the number of interfaces along the heat flow direction indicating the diminishing effects of interface resistance.

4.4 ILSS

From the ILSS tests, see Fig. 7, it is observed that the externally applied AC field greatly affects the influence of the GO filler on the matrix-fibre stress transfer properties. Initially, as expected and as reported previously [6], a dependency from the filler content is seen for both random GO and aligned GO CFRP samples. The sharp increase at low filler contents, 0.5 wt% and 1 wt%, is attributed to improved fracture resistance and toughness of the interlaminar regions leading to higher loading capabilities for the GO reinforced laminates. Both the morphology and shape (combination of planar geometry and wrinkled surface) and chemical composition of GO, i.e. the presence of oxygen groups that allow bonding with the epoxy matrix, have been highlighted as the predominant mechanisms for enhancing the mechanical properties of nanocomposites [22,55–57]. Considering the polymer dominated interlaminar regions, the ILSS is greatly improved by the addition of GO as the matrix properties have a significant influence on the fibre/matrix stress transfer of the laminate [58]. In general the addition of a high modulus filler into a low modulus matrix, like epoxy, allow to arrest or deflect the cracks initiated within the polymer medium [59]. Since the ILSS is designed to target these polymer-rich regions, improvements in the ILSS signify enhanced fracture toughness of the polymer matrix. Furthermore, it is known that laminate-level in-plane strengths are increased, and damage propagation is delayed due to the presence of tougher interlaminar regions [60,61].

The different behaviour observed for the A-GO/CFRP at high filler contents, above 2 wt%, is attributed to the reduction of the agglomeration due to electrostatic repulsive forces

between the GO flakes. As charge is accumulated on the edges of the GO flakes, adjacent flakes retract from forming aggregates and a chain-like network can be observed, see SEM images in Fig.4. Hence, the A-GO/CFRP laminates retain higher ILSS values at high filler contents compared to the laminates containing randomly oriented GO. This type of network is reminiscent of the z-pinning method that has been introduced as a means of enhancing the through-thickness mechanical properties of FRP laminates, but without the need of adding metallic pins within the laminate [29].

It is worth to note that the proposed methodology is applied to unidirectional CFRPs. ILSS values for such composites is low but they are relatively cheap to produce and large parts, e.g. wind turbine blades, can be manufactures using vacuum infusion. An application of the AC electric field combined with the addition of GO is relatively straightforward for such large structures and it allows to improve ILSS significantly.

5 Conclusions

An AC electric field was utillised to align GO flakes in the epoxy matrix of unidirectional CFRP laminates to increase the through-thickness electrical and thermal conductivity as well as the ILSS. Chain-like paths were formed through the polymer-rich layers facilitating the electrical current and heat conduction. Compared to laminates containing randomly oriented GO filler, improvements are seen at lower filler contents for both electrical and thermal conductivity. The electrical conduction mechanism appears to be significantly affected by the alignment process of the GO flakes. The thermal conductivity of A-GO/CFRP, albeit improved, does not show the same rate of improvement as the electrical conductivity, likely due to the high thermal interfacial resistance between GO and polymer.

It was also demonstrated that the use of an external AC field can be beneficial for the adoption of nano particle enhanced materials for industrial scale applications, as with a

relatively low field (30 V/mm) significant improvements in the functional (electrical, thermal) and mechanical properties (ILSS) can be realised. Besides the improved properties of the composite system, the electric field alignment process is also advantageous from a manufacturing standpoint, as a much lower filler content is required to obtain similar improvements as obtainable for random oriented filler systems. By utilising less filler in the polymer matrix, a lower viscosity can be achieved which significantly enhances the processability during infusion and injection processes.

Acknowledgments

The work was sponsored by the Marie Sklodowska Curie Actions, Innovative Training Networks (ITN), Call: H2020-MSCA-ITN-2014, as part of the 642771 SPARCARB project. The authors would like to thank Garmor Inc. (http://www.garmortech.com/) for providing the GO filler and Leuna Harze (https://www.leuna-harze.de/) for kindly supplying the epoxy resin used in this study.

References

1. Forintos N, Czigany T. Multifunctional application of carbon fiber reinforced polymer composites: Electrical properties of the reinforcing carbon fibers – A short review. *Compos Part B Eng*. 2019;162:331-343. doi:10.1016/J.COMPOSITESB.2018.10.098
2. Hung P, Lau K, Fox B, Hameed N, Lee JH, Hui D. Surface modification of carbon fibre using graphene–related materials for multifunctional composites. *Compos Part B Eng*. 2018;133:240-257. doi:https://doi.org/10.1016/j.compositesb.2017.09.010
3. Stankovich S, Dikin DA, Dommett GHB, et al. Graphene-based composite materials. *Nature*. 2006;442(7100):282.
4. Hill RF, Supancic PH. Thermal Conductivity of Platelet-Filled Polymer Composites. *J Am Ceram Soc*. 2002;85(4):851-857. doi:10.1111/j.1151-2916.2002.tb00183.x
5. Pozegic TR, Anguita J V, Hamerton I, et al. Multi-functional carbon fibre composites using carbon nanotubes as an alternative to polymer sizing. *Sci Rep*. 2016;6:37334.
6. Senis EC, Golosnoy IO, Dulieu-Barton JM, Thomsen OT. Enhancement of the electrical and thermal properties of unidirectional carbon fibre/epoxy laminates through the addition of graphene oxide. *J Mater Sci*. 2019:1-16. doi:10.1007/s10853-019-03522-8
7. Kim SY, Jang HG, Yang C-M, Yang BJ. Multiscale prediction of thermal conductivity

for nanocomposites containing crumpled carbon nanofillers with interfacial characteristics. *Compos Sci Technol*. 2018;155:169-176. doi:https://doi.org/10.1016/j.compscitech.2017.12.011

8. Han S, Lin JT, Yamada Y, Chung DDL. Enhancing the thermal conductivity and compressive modulus of carbon fiber polymer–matrix composites in the through-thickness direction by nanostructuring the interlaminar interface with carbon black. *Carbon N Y*. 2008;46(7):1060-1071.

9. El Sawi I, Olivier PA, Demont P, Bougherara H. Processing and electrical characterization of a unidirectional CFRP composite filled with double walled carbon nanotubes. *Compos Sci Technol*. 2012;73(1):19-26. doi:10.1016/j.compscitech.2012.08.016

10. Kandare E, Khatibi AA, Yoo S, et al. Improving the through-thickness thermal and electrical conductivity of carbon fibre/epoxy laminates by exploiting synergy between graphene and silver nano-inclusions. *Compos Part A Appl Sci Manuf*. 2015;69:72-82. doi:10.1016/j.compositesa.2014.10.024

11. Chu J, Young RJ, Slater TJAA, et al. Realizing the theoretical stiffness of graphene in composites through confinement between carbon fibers. *Compos Part A Appl Sci Manuf*. 2018;113:311-317. doi:https://doi.org/10.1016/j.compositesa.2018.07.032

12. Wang F, Cai X. Improvement of mechanical properties and thermal conductivity of carbon fiber laminated composites through depositing graphene nanoplatelets on fibers. *J Mater Sci*. 2019;54(5):3847-3862. doi:10.1007/s10853-018-3097-3

13. Stankovich S, Dikin DA, Dommett GHB, et al. Graphene-based composite materials. *Nature*. 2006;442(7100):282.

14. Mu M, Wan C, McNally T. Thermal conductivity of 2D nano-structured graphitic materials and their composites with epoxy resins. *2D Mater*. 2017;4(4):42001. doi:10.1088/2053-1583/aa7cd1

15. Marsden AJ, Papageorgiou DG, Vallés C, et al. Electrical percolation in graphene–polymer composites. *2D Mater*. 2018;5(3):32003. doi:10.1088/2053-1583/aac055

16. Li B, Dong S, Wu X, Wang C, Wang X, Fang J. Anisotropic thermal property of magnetically oriented carbon nanotube/graphene polymer composites. *Compos Sci Technol*. 2017;147:52-61. doi:10.1016/J.COMPSCITECH.2017.05.006

17. Wu S, Ladani RB, Zhang J, et al. Aligning multilayer graphene flakes with an external electric field to improve multifunctional properties of epoxy nanocomposites. *Carbon N Y*. 2015;94:607-618. doi:10.1016/J.CARBON.2015.07.026

18. Goh PS, Ismail AF, Ng BC. Directional alignment of carbon nanotubes in polymer matrices: Contemporary approaches and future advances. *Compos Part A Appl Sci Manuf*. 2014;56:103-126. doi:https://doi.org/10.1016/j.compositesa.2013.10.001

19. Heremans J, Beetz CP. Thermal conductivity and thermopower of vapor-grown graphite fibers. *Phys Rev B*. 1985;32(4):1981-1986. http://link.aps.org/doi/10.1103/PhysRevB.32.1981.

20. Liu ZZ, Peng P, Liu ZZ, et al. Electric-field-induced out-of-plane alignment of clay in poly (dimethylsiloxane) with enhanced anisotropic thermal conductivity and mechanical properties. *Compos Sci Technol*. 2018;165:39-47.

21. Wu S, Ladani RB, Ravindran AR, et al. Aligning carbon nanofibres in glass-fibre/epoxy composites to improve interlaminar toughness and crack-detection capability. *Compos Sci Technol*. 2017;152(Supplement C):46-56. doi:https://doi.org/10.1016/j.compscitech.2017.09.007

22. Young RJ, Kinloch IA, Gong L, Novoselov KS. The mechanics of graphene nanocomposites: A review. *Compos Sci Technol*. 2012;72(12):1459-1476. doi:10.1016/J.COMPSCITECH.2012.05.005

23. Remillard EM, Zhang Q, Sosina S, Branson Z, Dasgupta T, Vecitis CD. Electric-field alignment of aqueous multi-walled carbon nanotubes on microporous substrates. *Carbon N Y*. 2016;100:578-589. doi:10.1016/J.CARBON.2016.01.024

24. Morais MVC, Oliva-Avilés AI, Matos MAS, et al. On the effect of electric field application during the curing process on the electrical conductivity of single-walled carbon nanotubes–epoxy composites. *Carbon N Y*. April 2019. doi:10.1016/J.CARBON.2019.04.087

25. Mahmood H, Vanzetti L, Bersani M, Pegoretti A. Mechanical properties and strain monitoring of glass-epoxy composites with graphene-coated fibers. *Compos Part A Appl Sci Manuf*. 2018;107:112-123. doi:https://doi.org/10.1016/j.compositesa.2017.12.023

26. Tamrakar S, An Q, Thostenson ET, Rider AN, Haque BZ, Gillespie Jr JW. Tailoring interfacial properties by controlling carbon nanotube coating thickness on glass fibers using electrophoretic deposition. *ACS Appl Mater Interfaces*. 2016;8(2):1501-1510.

27. Sun W, Tomita H, Hasegawa S, Kitamura Y, Nakano M, Suehiro J. An array of interdigitated parallel wire electrodes for preparing a large-scale nanocomposite film with aligned carbon nanotubes. *J Phys D Appl Phys*. 2011;44(44):445303. doi:10.1088/0022-3727/44/44/445303

28. Ren Z, Lan Y, Wang Y. *Aligned Carbon Nanotubes: Physics, Concepts, Fabrication and Devices*. Springer Science & Business Media; 2012. doi:https://doi.org/10.1007/978-3-642-30490-3

29. Mouritz AP. Review of z-pinned composite laminates. *Compos Part A Appl Sci Manuf*. 2007;38(12):2383-2397. doi:10.1016/J.COMPOSITESA.2007.08.016

30. Grigoriou K, Ladani RB, Mouritz AP. Electrical properties of multifunctional Z-pinned sandwich composites. *Compos Sci Technol*. 2019;170:60-69. doi:https://doi.org/10.1016/j.compscitech.2018.11.030

31. Dransfield K, Baillie C, Mai Y-W. Improving the delamination resistance of CFRP by stitching—a review. *Compos Sci Technol*. 1994;50(3):305-317. doi:https://doi.org/10.1016/0266-3538(94)90019-1

32. Gaztelumendi I, Chapartegui M, Seddon R, Flórez S, Pons F, Cinquin J. Enhancement of electrical conductivity of composite structures by integration of carbon nanotubes via bulk resin and/or buckypaper films. *Compos Part B Eng*. 2017;122:31-40.

33. Zhang X, Fan X, Yan C, et al. Interfacial microstructure and properties of carbon fiber composites modified with graphene oxide. *ACS Appl Mater Interfaces*. 2012;4(3):1543-1552.

34. Yao X, Gao X, Jiang J, Xu C, Deng C, Wang J. Comparison of carbon nanotubes and

graphene oxide coated carbon fiber for improving the interfacial properties of carbon fiber/epoxy composites. *Compos Part B Eng*. 2018;132:170-177. doi:10.1016/J.COMPOSITESB.2017.09.012

35. Yao X, Hawkins SC, Falzon BG. An advanced anti-icing/de-icing system utilizing highly aligned carbon nanotube webs. *Carbon N Y*. 2018;136:130-138. doi:https://doi.org/10.1016/j.carbon.2018.04.039

36. Vryonis O, Andritsch T, Vaughan AS, Lewin PL. An alternative synthesis route to graphene oxide: influence of surface chemistry on charge transport in epoxy-based composites. *J Mater Sci*. 2019. doi:10.1007/s10853-019-03477-w

37. Monti M, Natali M, Torre L, Kenny JM. The alignment of single walled carbon nanotubes in an epoxy resin by applying a DC electric field. *Carbon N Y*. 2012;50(7):2453-2464. doi:https://doi.org/10.1016/j.carbon.2012.01.067

38. Ma C, Zhang W, Zhu Y, et al. Alignment and dispersion of functionalized carbon nanotubes in polymer composites induced by an electric field. *Carbon N Y*. 2008;46(4):706-710. doi:https://doi.org/10.1016/j.carbon.2008.01.019

39. Prasse T, Cavaillé J-Y, Bauhofer W. Electric anisotropy of carbon nanofibre/epoxy resin composites due to electric field induced alignment. *Compos Sci Technol*. 2003;63(13):1835-1841. doi:https://doi.org/10.1016/S0266-3538(03)00019-8

40. Lim C-S, Rodriguez AJ, Guzman ME, Schaefer JD, Minaie B. Processing and properties of polymer composites containing aligned functionalized carbon nanofibers. *Carbon N Y*. 2011;49(6):1873-1883. doi:https://doi.org/10.1016/j.carbon.2011.01.010

41. Schwarz M-K, Bauhofer W, Schulte K. Alternating electric field induced agglomeration of carbon black filled resins. *Polymer (Guildf)*. 2002;43(10):3079-3082. doi:https://doi.org/10.1016/S0032-3861(02)00084-8

42. Casalini R, Corezzi S, Livi A, Levita G, Rolla PA. Dielectric parameters to monitor the crosslink of epoxy resins. *J Appl Polym Sci*. 1997;65(1):17-25.

43. Osazuwa O, Vasileiou AA, Kontopoulou M, Docoslis A. Electric-field induced filler association dynamics and resulting improvements in the electrical conductivity of polyester/multiwall carbon nanotube composites. *Polym Compos*. 2017;38(8):1571-1578. doi:10.1002/pc.23724

44. Sengezer EC, Seidel GD, Bodnar RJ. Phenomenological characterization of fabrication of aligned pristine-SWNT and COOH-SWNT nanocomposites via dielectrophoresis under AC electric field. *Polym Compos*. 2015;36(7):1266-1279. doi:10.1002/pc.23031

45. Lubineau G, Rahaman A. A review of strategies for improving the degradation properties of laminated continuous-fiber/epoxy composites with carbon-based nanoreinforcements. *Carbon N Y*. 2012;50(7):2377-2395. doi:https://doi.org/10.1016/j.carbon.2012.01.059

46. ASTM D2344/D2344M-16 ASTM International West Conshohocken PA 2016 www.astm.org STM for S-BS of PMCM and TL. ASTM D2344 / D2344M-16, Standard Test Method for Short-Beam Strength of Polymer Matrix Composite Materials and Their Laminates, ASTM International, West Conshohocken, PA, 2016, www.astm.org. doi:10.1520/D2344_D2344M-16

47. Tuinstra F, Koenig JL. Raman Spectrum of Graphite. *J Chem Phys*. 1970;53(3):1126-

1130. doi:10.1063/1.1674108

48. Pimenta MA, Dresselhaus G, Dresselhaus MS, Cançado LG, Jorio A, Saito R. Studying disorder in graphite-based systems by Raman spectroscopy. *Phys Chem Chem Phys*. 2007;9(11):1276-1290. doi:10.1039/B613962K

49. Venugopal G, Jung M-H, Suemitsu M, Kim S-J. Fabrication of nanoscale three-dimensional graphite stacked-junctions by focused-ion-beam and observation of anomalous transport characteristics. *Carbon N Y*. 2011;49(8):2766-2772. doi:10.1016/J.CARBON.2011.03.003

50. Chen H, Ginzburg V V., Yang J, et al. Thermal conductivity of polymer-based composites: Fundamentals and applications. *Prog Polym Sci*. 2016;59:41-85. doi:10.1016/J.PROGPOLYMSCI.2016.03.001

51. Kostagiannakopoulou C, Fiamegkou E, Sotiriadis G, Kostopoulos V. Thermal Conductivity of Carbon Nanoreinforced Epoxy Composites. *J Nanomater*. 2016;2016. doi:10.1155/2016/1847325

52. Chen H, Ginzburg V V., Yang J, et al. Thermal conductivity of polymer-based composites: Fundamentals and applications. *Prog Polym Sci*. 2016;59:41-85. http://www.sciencedirect.com/science/article/pii/S0079670016000216. Accessed September 28, 2018.

53. Liu Z, Peng P, Liu Z, et al. Electric-field-induced out-of-plane alignment of clay in poly(dimethylsiloxane) with enhanced anisotropic thermal conductivity and mechanical properties. *Compos Sci Technol*. 2018;165:39-47. doi:10.1016/J.COMPSCITECH.2018.06.015

54. Su Y, Li JJ, Weng GJ. Theory of thermal conductivity of graphene-polymer nanocomposites with interfacial Kapitza resistance and graphene-graphene contact resistance. *Carbon N Y*. 2018;137:222-233. doi:10.1016/j.carbon.2018.05.033

55. Rafiee MA, Rafiee J, Wang Z, Song H, Yu Z-Z, Koratkar N. Enhanced mechanical properties of nanocomposites at low graphene content. *ACS Nano*. 2009;3(12):3884-3890.

56. Surnova A, Balkaev D, Musin D, Amirov R, Dimiev AM. Fully exfoliated graphene oxide accelerates epoxy resin curing, and results in dramatic improvement of the polymer mechanical properties. *Compos Part B Eng*. 2019;162:685-691. doi:10.1016/J.COMPOSITESB.2019.01.020

57. Jayan JS, Saritha A, Joseph K. Innovative materials of this era for toughening the epoxy matrix: A review. *Polym Compos*. 2018;39(S4):E1959-E1986. doi:10.1002/pc.24789

58. Ramos-Fernandez G, Muñoz M, García-Quesada JC, Rodriguez-Pastor I, Martin-Gullon I. Role of graphene oxide surface chemistry on the improvement of the interlaminar mechanical properties of resin infusion processed epoxy-carbon fiber composites. *Polym Compos*. 2018;39(S4):E2116-E2124. doi:10.1002/pc.24478

59. Atif R, Shyha I, Inam F. Mechanical, thermal, and electrical properties of graphene-epoxy nanocomposites—A review. *Polymers (Basel)*. 2016;8(8):281.

60. Guzman de Villoria R, Hallander P, Ydrefors L, Nordin P, Wardle BL. In-plane strength enhancement of laminated composites via aligned carbon nanotube

interlaminar reinforcement. *Compos Sci Technol*. 2016;133:33-39. doi:https://doi.org/10.1016/j.compscitech.2016.07.006

61. Blanco J, García EJ, Guzmán de Villoria R, Wardle BL. Limiting Mechanisms of Mode I Interlaminar Toughening of Composites Reinforced with Aligned Carbon Nanotubes. *J Compos Mater*. 2009;43(8):825-841. doi:10.1177/0021998309102398